

# New Crosslinkable Hole Conductors for Blue-Phosphorescent Organic Light-Emitting Diodes\*\*

Philipp Zacharias, Malte C. Gather, Markus Rojahn, Oskar Nuyken, and Klaus Meerholz\*

Owing to their low power consumption, light weight, fast response and wide viewing angle, organic light-emitting diodes (OLEDs) are promising for future lighting and display applications.<sup>[1]</sup> The preparation of OLEDs from solution (for example, by spin-coating) is often more favorable than by vacuum-deposition techniques, especially for the roll-to-roll production of large-area substrates. For the fabrication of efficient multilayer devices from solution, however, it is crucial that the underlying layers do not dissolve when depositing the next layer. This requirement can be fulfilled by introducing precursor materials with polymerizable moieties that are crosslinked after deposition. However, crosslinking often has a negative impact on the electrical properties of the material.<sup>[2]</sup> We previously introduced oxetane-functionalized derivatives of the hole conductor triphenylamine dimer (TPD) and of polyfluorene-based electroluminescent polymers.<sup>[3]</sup> We were able to show that thin layers of these materials can be crosslinked through photoinitiated cationic ring-opening polymerization (CROP) and, thus, rendered insoluble, without degrading their electrical properties.<sup>[4]</sup> The synthesis makes use of the fact that, while oxetanes are reactive under acidic conditions, they are stable even against strong bases.

Light emission in OLEDs is based on the radiative decay of excited states that are formed by the recombination of holes and electrons. According to fundamental spin statistics, the ratio of triplet to singlet states is 3:1. Thus, in singlet-state-emitting (fluorescent) materials, 75% of the excited states are lost. This loss can be avoided by the use of triplet-state-emitting (phosphorescent) transition-metal complexes.<sup>[5]</sup> Efficient charge injection into the emissive layer requires the use of one or several layers of hole- and electron-transporting materials.<sup>[6,7]</sup>

We previously reported on the synthesis, characterization, and application of oxetane-functionalized crosslinkable TPDs (XTPDs) with HOMO energies ( $E_{\text{HOMO}}$ ) between  $-5.1$  and  $-5.3$  eV (relative to vacuum).<sup>[8]</sup> In combination with many fluorescent materials and with red- or green-phosphorescent materials, OLEDs containing hole-transport layers (HTL) of these XTPDs have an exceptional performance profile.<sup>[7]</sup> However, the concept has not yet been very successful for blue triplet-state emitters, mainly because of insufficient hole injection into the HOMO of these materials, which is typically located at around  $-6$  eV.<sup>[6]</sup>

Herein, we report on the synthesis, thermomechanical properties, and electrochemistry of a series of new XTPDs with HOMO energies down to  $-5.8$  eV. We use these XTPDs to fabricate efficient blue-electrophosphorescent OLEDs and show that the luminous efficiency of the devices correlates directly with the HOMO energy of the XTPD.

The new XTPDs (**1–12**, Scheme 1) were synthesized by palladium-catalyzed aromatic amination (Hartwig–Buchwald reaction) from the corresponding benzidine derivatives and bromoarenes (if necessary, two different bromoarenes).<sup>[9]</sup> The higher reactivity of primary amines compared to secondary amines in the Hartwig–Buchwald reaction was exploited for selectivity.

The alkyl ether unit between the aromatic system and the oxetane ring acts simultaneously as a linker and as a spacer, providing flexibility to the oxetane units and ensuring good solubility of the monomer. It also prevents crystallization, a function that is crucial for the formation of homogenous films. XTPDs with two alkyl ether–oxetane units have a glass-transition temperature ( $T_g$ ) of around  $0^\circ\text{C}$ ; those with four alkyl ether–oxetane units have a  $T_g$  value of around  $-30^\circ\text{C}$  (Table 1). Note that the oxidation potential and UV/Vis spectra of **11** and **12** are identical within the limits of accuracy. Thus, the number of alkyl ether–oxetane units influences the thermomechanical, but not the electrochemical and optical properties of the molecule. Upon crosslinking polymerization, the  $T_g$  value of the material rises sharply: poly-**12** has a  $T_g$  value of  $101^\circ\text{C}$ , whereas in the case of poly-**11** no glass transition is observed (up to  $300^\circ\text{C}$ ), probably because of a higher density of crosslinking.

To tune the HOMO energy of the XTPDs, we utilized two concepts: First, donor substituents, such as alkoxy or alkyl, were used to increase the HOMO energy, while acceptor substituents, such as chloro, fluoro,  $\text{CF}_3$ , or  $\text{SO}_2$ , were used to reduce the HOMO energy. Second, substituents at positions 2, 2', 6, and 6' of the biphenyl core were employed to introduce a large torsion angle between the two ring planes, which reduces the HOMO energy even further, owing to reduced electron delocalization.<sup>[10]</sup> To prevent oxidative

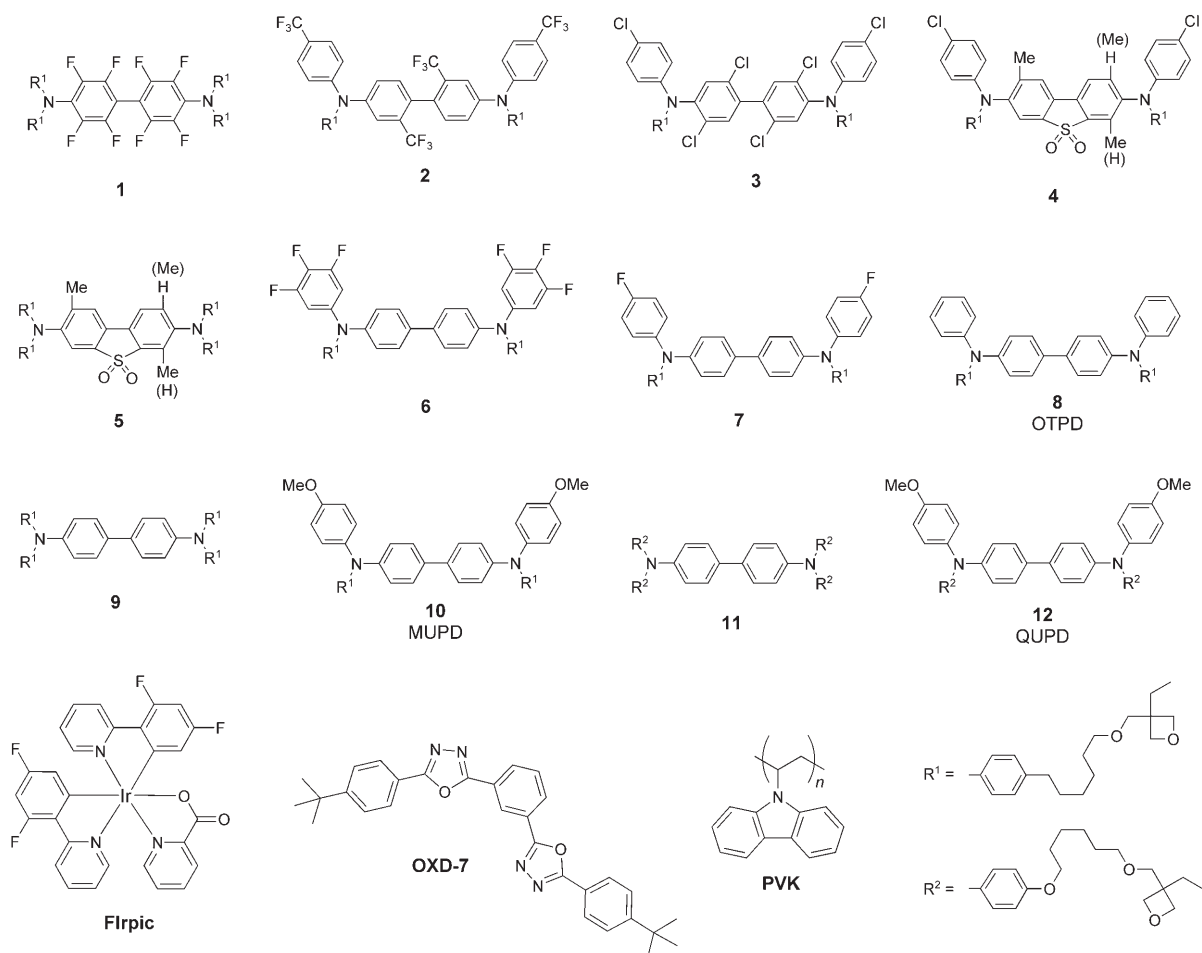
[\*] P. Zacharias, M. C. Gather, Prof. K. Meerholz  
Universität zu Köln  
Physikalische Chemie  
Luxemburger Strasse 116, 50939 Cologne (Germany)  
Fax: (+49) 211-470-5144  
E-mail: klaus.meerholz@uni-koeln.de

M. Rojahn, Prof. O. Nuyken  
Technische Universität München  
Lehrstuhl für Makromolekulare Stoffe  
Lichtenbergstrasse 4, 85747 Garching (Germany)

[\*\*] This work was supported by the Bundesministerium für Bildung und Forschung (BMBF). We thank Dr. Jürgen Steiger (Degussa, Marl) for the UPS data and Georgios Liaptsis (Universität zu Köln) for his help with the synthesis.



Supporting information for this article is available on the WWW under <http://www.angewandte.org> or from the author.



**Scheme 1.** The oxetane-functionalized XTPDs **1–12** and other components of the blue-phosphorescent OLEDs.

**Table 1:** Electrochemical and thermomechanical data for the XTPDs **1–12** and other components of the blue-phosphorescent OLEDs.

Component	$E_{ox}$ [V] <sup>[a]</sup>	$E_i$ [eV] <sup>[e]</sup>	$E_{HOMO}$ [eV] <sup>[b]</sup>	$T_g$ [°C]
<b>1</b>	0.79	5.80	−5.79	−26
<b>2</b>	0.77	5.95	−5.78	1
<b>3</b>	0.74	5.80	−5.75	7
<b>4</b>	0.63	5.50	−5.65	−2
<b>5</b>	0.49	5.50	−5.53	−27
<b>6</b>	0.46	–	−5.50	−1
<b>7</b>	0.28	–	−5.34	0
<b>8</b>	0.24	5.45	−5.30	−5
<b>9</b>	0.19	5.40	−5.26	−34
<b>10</b>	0.13	5.10	−5.21	−1
<b>11</b>	0.08	–	−5.16	−27
<b>12</b>	0.07	5.25	−5.15	−1
PVK	≥ 0.80 <sup>[c]</sup>	–	−5.84 <sup>[d]</sup>	≈ 200
OXD-7	–	–	−6.30 <sup>[13]</sup>	–
Flrpic	0.90	–	−5.89	–
PEDOT	–	5.10	−5.10 <sup>[14]</sup>	–

[a] All compounds showed reversible redox behavior. [b] Calculated from  $E_{ox}$  according to Equation (1). [c] Irreversible. [d] Determined according to the extrapolation method developed herein. [e] Measured by UPS.

dimerization, all the XTPDs with substituents on the biphenyl core were designed such that the positions on the outer phenyl rings *para* to the nitrogen atoms are blocked (by alkyl,

$CF_3$ , or chloro substituents).<sup>[11]</sup> We point out that by changing the substitution pattern, not only the HOMO energy is altered, but also the hole mobility. However, this effect cannot be rationalized as easily because, among other factors, the morphology of the hole-transporting material plays an important role.

Cyclic voltammetry (CV) and UV photoelectron spectroscopy (UPS) were used to obtain information about the HOMO energies of the different XTPDs. CV determines the oxidation potential ( $E_{ox}$ ) as the energy that is necessary to remove an electron from the molecule when it is surrounded by solvent and in the presence of an electrolyte. UPS measures the ionization potential ( $E_i$ ) as the energy required to remove this electron from a molecule at the surface of a solid to the vacuum. Although  $E_{ox}$  and  $E_i$  are related, the exact correlation varies for different experimental setups and for different kinds of molecules.

The oxidation potential of the compounds **1–12** was measured by CV in  $CH_2Cl_2$  (Table 1). The experimental error is around  $\pm 10$  mV. The reliability of UPS measurements is generally lower ( $\Delta E_i = \pm 100$  mV).<sup>[6]</sup> Therefore, we used our UPS data merely to determine the correlation between  $E_i$  and  $E_{ox}$ , and then calculated  $E_{HOMO}$  ( $= -E_i$ ) from the  $E_{ox}$  values (Table 1). We found the linear correlation expressed by Equation (1). It is important to note that this correlation

$$E_i = (5.1 \pm 0.05) \text{ eV} + E_{\text{ox}} \times (0.9 \pm 0.1) \text{ eV V}^{-1} \quad (1)$$

depends on the polarity of the CV solvent. This effect becomes apparent in the dependence we found for the  $E_{\text{ox}}$  values in  $\text{CH}_2\text{Cl}_2$  and in  $\text{CH}_3\text{CN}$  [Eq. (2)].

$$E_{\text{ox}}^{\text{CH}_3\text{CN}} = (0.12 \pm 0.01) \text{ V} + E_{\text{ox}}^{\text{CH}_2\text{Cl}_2} (0.84 \pm 0.02) \quad (2)$$

To demonstrate that the XTPDs can improve hole injection in blue-phosphorescent devices, we fabricated a series of OLEDs comprising one or three layers of the different XTPDs and a layer of the blue phosphor FIrpic in a matrix of PVK and the electron conductor OXD-7 (Scheme 1). The devices had the following structure (Figure 1): ITO/PEDOT:PSS (35 nm)/XTPDs (each 8 nm)/PVK:OXD-7:FIrpic (67:28:5 wt %; 75 nm)/CsF (4 nm)/Al (70 nm).<sup>[7,12]</sup>

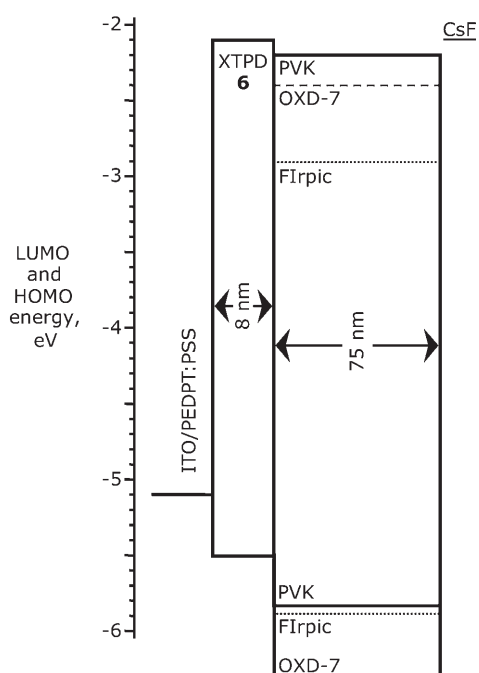


**Figure 1.** The layer arrangement in the OLED with XTPD 6. The LUMO and HOMO energies of the components are indicated by horizontal lines. ITO = indium tin oxide, PEDOT = poly(3,4-ethylenedioxythiophene), PSS = poly(styrenesulfonate).

In Figure 2 and Table 2, the data for some of the devices, as well as literature data, are compared. Our reference device (without an XTPD layer) achieves a maximum luminous efficiency ( $\text{LE}_{\text{max}}$ ) of  $17 \text{ cd A}^{-1}$  at a brightness of  $700 \text{ cd m}^{-2}$ . These results are in reasonable agreement with recent studies on similar devices: Yang et al. reported a maximum luminous efficiency of  $18 \text{ cd A}^{-1}$  at  $200 \text{ cd m}^{-2}$ .<sup>[13]</sup> Mathai et al. reported higher peak efficien-

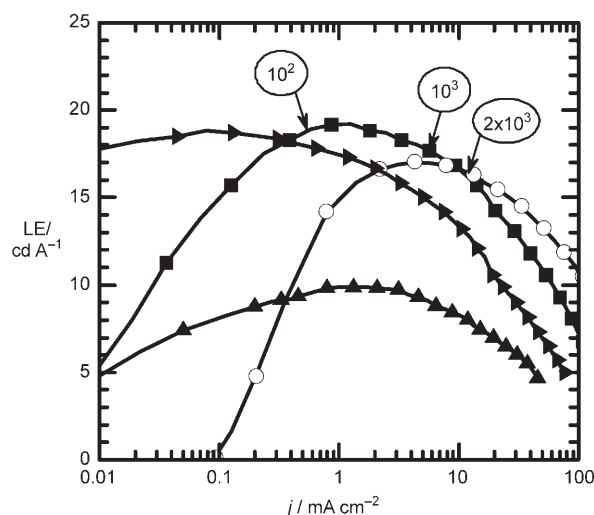


**Figure 2.** Luminous efficiency (LE) versus current density ( $j$ ) for the blue-phosphorescent OLEDs without ( $\circ$ ) and with XTPDs ( $\blacksquare$  6,  $\blacktriangle$  12/8/6,  $\blacktriangle$  8/6/4). The numbers in circles correspond to the brightness ( $j \times \text{LE}$ ) of the device ( $\blacksquare$ ) in  $\text{cd m}^{-2}$ .

cies of  $22 \text{ cd A}^{-1}$ ; however, the maximum luminous efficiency occurred at a very low brightness ( $26 \text{ cd m}^{-2}$ ), and the efficiency decayed to  $20 \text{ cd A}^{-1}$  at  $700 \text{ cd m}^{-2}$ .<sup>[14]</sup> We attribute the 15% difference in the luminous efficiency of our reference device to a residual electron-injection barrier, which could be overcome by further optimization of the CsF cathode.

For practical brightness levels (less than  $2000 \text{ cd m}^{-2}$ ), the efficiency is significantly enhanced if a single HTL of 6 is integrated into the device (Figure 2). Compared to that of the reference device without an HTL ( $17 \text{ cd A}^{-1}$ ), the peak efficiency is increased ( $19.2 \text{ cd A}^{-1}$ ). At the same time, the turn-on voltage ( $L_{\text{on}}$ ) of the electroluminescence is reduced by 1.3 V from that of the reference, to 3.1 V (Table 2).

Below  $0.4 \text{ mA cm}^{-2}$  (or  $70 \text{ cd m}^{-2}$ ), the best luminous efficiency was obtained for a device with three XTPD layers (12/8/6). It is important to note that the efficiency of the 8/6/4-triple-HTL device is lower than that of the 6-single-HTL device, although the injection barrier for holes in the triple-HTL device is divided into even smaller steps (Figures 1 and 2). Also note that, as predicted by optical modeling, the

**Table 2:** Characteristics of the OLEDs without and with XTPDs as HTLs.

HTL	$\text{LE}_{\text{max}}^{[a]}$ [ $\text{cd A}^{-1}$ ]	$U$ [V]	$\text{LE}_{1000 \text{ cd m}^{-2}}^{[a]}$ [ $\text{cd A}^{-1}$ ]	$U$ [V]	$\text{PE}_{\text{max}}^{[b]}$ [ $\text{lm W}^{-1}$ ]	$U$ [V]	$L_{\text{on}}^{[c]}$ [V]	$x/y^{[d]}$
6	19.2	6.3	17.7	8.1	10.2	5.4	3.1	0.170/0.365
8/6/4	9.9	7.8	7.9	11.3	4.9	4.5	3.0	0.165/0.360
12/8/6	18.8	4.5	14.3	8.9	15.4	3.6	2.7	0.165/0.360
–	17.0	7.2	16.9	7.5	7.9	6.6	4.4	0.170/0.370
12/8 <sup>[7]</sup>	11.5	7.2	9.3	11.0	8.0	5.5	3.0	–
– <sup>[7]</sup>	15.0	6.7	13.1	9.1	7.2	5.7	4.8	–
– <sup>[14]</sup>	22.0	5.6	19.0	7.7	14.0	4.9	–	0.170/0.370

[a] Luminous efficiency at voltage  $U$ , error:  $\pm 0.1 \text{ cd A}^{-1}$ . [b] Power efficiency at voltage  $U$ , error:  $\pm 0.1 \text{ lm W}^{-1}$ . [c] Turn-on voltage (brightness greater than  $10^{-2} \text{ cd m}^{-2}$ ). [d] Color coordinates (Commission Internationale de l'Éclairage (CIE)), error:  $\pm 0.005$ .

electroluminescence shifts to blue with increasing number of XTPD layers, as revealed by the color coordinates in Table 2.

In Figure 3, we plot the maximum luminous efficiencies of all the single-HTL OLEDs as a function of the HOMO energy of the respective XTPD. A distinct efficiency maximum is observed for **6**, while the luminous efficiency falls off for higher and lower HOMO energies. In agreement with our

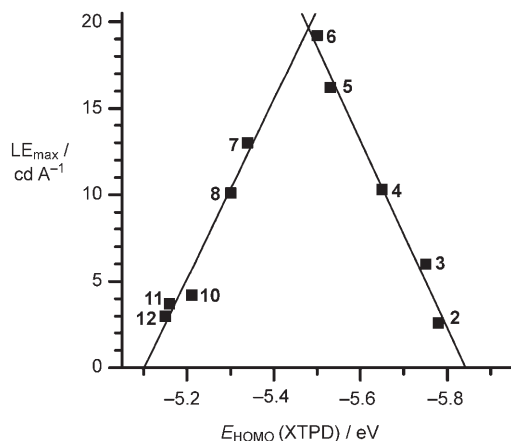


**Figure 3.** Maximum luminous efficiency ( $LE_{\text{max}}$ ) of the single-HTL OLEDs versus the HOMO energy ( $E_{\text{HOMO}}$ ) of the corresponding XTPD. The lines indicate linear fits for **2–6** and for **7, 8, 10–12**, respectively. See the Supporting Information for the corresponding LE versus  $j$  plots.

expectations, the maximum lies exactly halfway between the HOMO energies of PEDOT:PSS and PVK. At this point, the hole-injection barrier is split into two equally large steps. Surprisingly, the correlation between the HOMO energy of the XTPD and luminous efficiency of the OLED is linear on both sides of the maximum. This result allows us to extrapolate to a device containing an HTL with a HOMO level matching one of the adjacent layers, that is, PEDOT:PSS (upper limit) or PVK (lower limit). The resulting value of  $E_{\text{HOMO}} = -5.1$  eV for PEDOT:PSS agrees perfectly with values reported in the literature.<sup>[15]</sup> Owing to irreversible oxidation during the CV measurement, the oxidation potential of PVK is not directly accessible electrochemically. However, according to the extrapolation in Figure 3, a value of  $E_{\text{HOMO}} = -5.85$  eV is expected. We believe that this experiment provides a unique method to measure the HOMO energy of PVK.

To summarize, the synthesis of XTPDs with HOMO energies down to  $-5.8$  eV allowed us to fabricate efficient phosphorescent OLEDs with improved device performance. Devices containing five organic layers were produced through a solution process. As the oxetane units in the compounds we investigated are effectively separated from the electrooptically active moieties, most of our conclusions can be transferred to TPDs in general.

## Experimental Section

**Hartwig–Buchwald coupling:** The appropriate bromoarene (2.2 equiv) and NaOtBu (1.5 equiv per reacting NH) were added to a solution of the corresponding diamine in dry toluene (20 mL per mmol diamine) under argon. The catalyst was freshly prepared in an  $\text{N}_2$ -filled glovebox from  $[\text{Pd}_2\text{dba}_3]$  (dba = dibenzylideneacetone; Pd/N 0.02:1) and  $\text{PrBu}_3$  (P/Pd = 0.8; Aldrich, 98%) dissolved in dry toluene. Before adding the catalyst, the solution was degassed rigorously and heated to the reaction temperature (25–110 °C, depending on the reaction). The completion of the reaction was checked by TLC or ESI-MS (10- $\mu\text{L}$  samples quenched with methanol). Then, the mixture was diluted 1:1 with *tert*-butyl methyl ether (TBME), washed with water, extracted with TBME, and dried over  $\text{MgSO}_4$ . Evaporation of the solvent and purification of the resulting oil by medium-pressure liquid chromatography (MPLC; toluene/ethyl acetate on silica, 20 mL  $\text{min}^{-1}$ ), followed by microfiltration (ethyl acetate over 0.45- $\mu\text{m}$  poly(vinylidene fluoride) PVDF) and vacuum drying ( $10^{-5}$  bar), yielded the products in yields of 44–84%. The purity of all the compounds was confirmed with  $^1\text{H}$ ,  $^{13}\text{C}$ , and  $^{19}\text{F}$  NMR spectroscopy (Bruker, 300 MHz,  $\text{CDCl}_3$ ), ESI-MS (Thermo Finnigan MAT 900ST), and elemental analysis. The glass-transition temperatures were determined by differential scanning calorimetry (DSC; Mettler Toledo DSC821<sup>e</sup>), using the identical second and third heating cycles. Cyclic voltammograms were recorded on a potentiostat/galvanostat (EG + G Instruments M283) in  $\text{CH}_2\text{Cl}_2$  solution ( $10^{-3}$  M) containing  $\text{NBu}_4\text{PF}_6$  ( $10^{-1}$  M) as electrolyte. The potentials cited are given versus the ferrocene/ferrocenium redox couple. UPS was performed on a Riken AC-2 spectrometer.

**OLED fabrication:** The OLEDs were fabricated on ITO-coated glass substrates. The substrates were thoroughly cleaned and treated with  $\text{O}_3$ . A layer of PEDOT:PSS (35 nm, Baytron P, AI4083, H. C. Starck) was spin-coated onto the substrates and dried for 80 s at 110 °C. The substrates were transferred to an  $\text{N}_2$ -filled glovebox, and the XTPD layers were spin-coated onto them from toluene solutions (2–5  $\text{mg mL}^{-1}$ ) containing 4-octyloxydiphenyliodonium hexafluoroantimonate (OPPI; 4.0 mol%) as photoinitiator. The films were irradiated with UV light (360 nm) for 10 s and cured at 100 °C for 60 s to promote crosslinking.<sup>[8]</sup> A blend of PVK, OXD-7 (28 wt%), and Firpic (5 wt%) dissolved in chlorobenzene (15  $\text{mg mL}^{-1}$ ) was spin-coated onto the XTPD layer(s). Subsequently, the cathode was deposited by thermal evaporation (at 10.9 bar). Current–voltage–luminescence characteristics were measured with an amperometer (Keithley 2400) and a calibrated photodiode.

Received: December 14, 2006

Published online: May 4, 2007

**Keywords:** charge-carrier injection · electrochemistry · electrophosphorescence · light-emitting diodes · oxetanes

- [1] a) S. R. Forrest, *Nature* **2004**, *428*, 911; b) B. W. D'Andrade, S. R. Forrest, *Adv. Mater.* **2004**, *16*, 1585; c) A. Misra, P. Kumar, M. N. Kamalasanan, S. Chandra, *Semicond. Sci. Technol.* **2006**, *21*, R35.  
 [2] a) E. Bellmann, S. E. Shaheen, S. Thayumanavan, S. Barlow, R. H. Grubbs, S. R. Marder, B. Kippelen, N. Peyghambarian, *Chem. Mater.* **1998**, *10*, 1668; b) A. Bacher, P. G. Bentley, D. D. C. Bradley, L. K. Douglas, P. A. Glarvey, M. Grell, K. S. Whitehead, M. L. Turner, *J. Mater. Chem.* **1999**, *9*, 2985.  
 [3] a) M. S. Bayerl, T. Braig, O. Nuyken, D. C. Müller, M. Groß, K. Meerholz, *Macromol. Rapid Commun.* **1999**, *20*, 224; b) K. Meerholz, C. D. Müller, O. Nuyken in *Organic Light-Emitting Devices: Synthesis, Properties and Applications* (Eds.: K. Müllen, U. Scherf), Wiley-VCH, Weinheim, **2005**, p. 426.  
 [4] a) E. Bacher, S. Jungermann, M. Rojahn, V. Wiederhirn, O. Nuyken, *Macromol. Rapid Commun.* **2004**, *25*, 1191; b) C. D.

- Müller, A. Falcou, N. Reckefuss, M. Rojahn, V. Wiederhirn, P. Rudati, H. Frohne, O. Nuyken, H. Becker, K. Meerholz, *Nature* **2003**, *421*, 829; c) M. Gather, A. Köhnen, A. Falcou, H. Becker, K. Meerholz, *Adv. Funct. Mater.* **2007**, *17*, 191.
- [5] a) M. A. Baldo, D. F. O'Brien, Y. You, A. Shoustikov, S. Sibley, M. E. Thompson, S. R. Forrest, *Nature* **1998**, *395*, 151; b) Y. R. Sun, N. C. Giebink, H. Kanno, B. W. Ma, M. E. Thompson, S. R. Forrest, *Nature* **2006**, *440*, 908.
- [6] B. W. D'Andrade, S. Datta, S. R. Forrest, P. Djurovich, E. Polikarpov, M. E. Thompson, *Org. Electron.* **2005**, *6*, 11.
- [7] X. H. Yang, C. D. Müller, D. Neher, K. Meerholz, *Adv. Mater.* **2006**, *18*, 948.
- [8] D. C. Müller, T. Braig, H.-G. Nothofer, M. Arnoldi, M. Gross, U. Scherf, O. Nuyken, K. Meerholz, *ChemPhysChem* **2000**, *1*, 207.
- [9] a) A. R. Muci, S. L. Buchwald, *Top. Curr. Chem.* **2002**, *219*, 131; b) J. F. Hartwig in *Handbook of Organopalladium Chemistry for Organic Synthesis, Vol. 1* (Ed.: E. Negishi), Wiley, New York, **2002**, p. 1051; c) S. Thayumanavan, S. Barlow, S. R. Marder, *Chem. Mater.* **1997**, *9*, 3231.
- [10] P. J. Low, M. A. J. Paterson, D. S. Yufit, J. A. K. Howard, J. C. Cherryman, D. R. Tackley, R. Brook, B. Brown, *J. Mater. Chem.* **2005**, *15*, 2304.
- [11] P. J. Low, M. A. J. Paterson, A. E. Goeta, D. S. Yufit, J. A. K. Howard, J. C. Cherryman, D. R. Tackley, B. Brown, *J. Mater. Chem.* **2004**, *14*, 2516.
- [12] In contrast to reports in the literature, we found that 5 wt% FIrpic gives better luminous efficiency than 10 wt%.
- [13] X. H. Yang, F. Jaiser, S. Klinger, D. Neher, *Appl. Phys. Lett.* **2006**, *88*, 021107.
- [14] M. K. Mathai, V. E. Choong, S. A. Choulis, B. Krummacker, F. So, *Appl. Phys. Lett.* **2006**, *88*, 243512.
- [15] N. Koch, A. Kahn, J. Ghijsen, J. J. Pireaux, J. Schwartz, R. L. Johnson, A. Elschner, *Appl. Phys. Lett.* **2003**, *82*, 70.
-